Cloning, tissue distribution, pharmacology and three-dimensional modelling of melanocortin receptors 4 and 5 in rainbow trout suggest close evolutionary relationship of these subtypes

Tatjana HAITINA*, Janis KLOVINS*†, Jan ANDERSSON*, Robert FREDRIKSSON*, Malin C. LAGERSTRÖM*, Dan LARHAMMAR*, Earl T. LARSON‡ and Helgi B. SCHIÖTH*[1]

*Department of Neuroscience, Unit of Pharmacology, Uppsala University, BMC, Uppsala SE75124, Sweden, †Biomedical Research and Study Centre, University of Latvia, Riga LV1069, Latvia, and ‡Departments of Biology and Psychology, Northeastern University, Boston, MA 02115, U.S.A.

The rainbow trout (*Oncorhynchus mykiss*) is one of the most widely used fish species in aquaculture and physiological research. In the present paper, we report the first cloning, 3D (three-dimensional) modelling, pharmacological characterization and tissue distribution of two melanocortin (MC) receptors in rainbow trout. Phylogenetic analysis indicates that these receptors are orthologues of the human MC4 and MC5 receptors. We created 3D molecular models of these rainbow trout receptors and their human counterparts. These models suggest greater divergence between the two human receptors than between their rainbow trout counterparts. The pharmacological analyses demonstrated that ACTH (adrenocorticotropic hormone) had surprisingly high affinity for the rainbow trout MC4 and MC5 receptors, whereas α-, β- and γ-MSH (melanocyte-stimulating hormone) had lower affinity. In second-messenger studies, the cyclic MSH analogues MTII and SHU9119 acted as potent agonist and antagonist respectively at the rainbow trout MC4 receptor, indicating that these ligands are suitable for physiological studies in rainbow trout. Interestingly, we found that the rainbow trout MC4 receptor has a natural high-affinity binding site for zinc ions (0.5 μM) indicating that zinc may play an evolutionary conserved role at this receptor. Reverse transcription PCR indicates that the rainbow trout receptors are expressed both in peripheral tissues and in the central nervous system, including the telencephalon, optic tectum and hypothalamus. Overall, this analysis indicates that the rainbow trout MC4 and MC5 receptors have more in common than their mammalian counterparts, which may suggest that these two receptors have a closer evolutionary relationship than the other MC receptor subtypes.

Key words: adrenocorticotropic hormone (ACTH), G-protein-coupled receptor (GPCR), hormone receptor, melanocortin, melanocyte-stimulating hormone (MSH), rainbow trout (*Oncorhynchus mykiss*).

INTRODUCTION

The teleost fishes appeared about 150 million years ago in the late Jurassic period [1], long after the divergence of the gnathostome vertebrates. Today, there are over 20 000 teleost species identified [2]. Ray-finned teleost fishes have attracted increasing interest in biological research, and different species serve as widely studied model organisms for various reasons. Rainbow trout (*Oncorhynchus mykiss*) has proven to be very suitable for a variety of physiological experiments. The main advantages of the rainbow trout are that, due to the size of the animal, it is easy to isolate different tissues and cell types (reviewed in [3]), and it is very suitable for behavioural studies, including regulation of food intake. Rainbow trout is thus one of the most widely used species for studies on fish today. Rainbow trout is also important in aquaculture and popular in sport fishing.

The melanocortin (MC) peptides [4] mediate their effects through five MC receptors that belong to the rhodopsin family of GPCRs (G-protein-coupled receptors) [5], which represent the single most important class of drug targets. Each of these five MC receptors has a characteristic binding profile regarding the different pro-opiomelanocortin products [4]. The MC5 receptor has also been found centrally, although it is mainly expressed in a number of human peripheral tissues, including adrenal gland, adipocytes and leucocytes [6]. The functional properties of the MC5 receptor are, however, still not well understood, with the exception of its participation in exocrine function to regulate sebaceous gland secretion in mice [7]. Central MC signalling plays an important role in the regulation of energy homoeostasis in mammals. The critical role for the MC4 receptor in energy balance was demonstrated by target disruption of the MC4 receptor gene that induces hyperphagia and obesity in mice [8], and this receptor is now one of the best-characterized monogenic causes of obesity. Stimulation of the MC4 receptor reduces food intake [9], whereas blocking of the receptor causes very strong orexigenic effect [10]. The MC4 receptor is currently one of the most pursued targets for the development of drugs to treat obesity and anorexia.

Recent evidence indicates that the MC system in fish, including the MC4 receptors, is involved in the central regulation of energy balance, as in mammals [11–14]. The MC system thus seems to

Abbreviations used: 3D, three-dimensional; ACTH, adrenocorticotropic hormone; CNS, central nervous system; Dre, *Danio rerio* (zebrafish); Gga, *Gallus gallus* (domestic chicken); GPCR, G-protein-coupled receptor; Hsa, *Homo sapiens* (human); HS024, cyclic MSH analogue, c[acetyl-Cys^3,Nle^4,Arg^5,D-Nal^7,Cys-NH$_2$^{11}]α-MSH-(3–11); MC, melanocortin; Mmu, *Mus musculus* (house mouse); MSH, melanocyte-stimulating hormone; MTII, cyclic MSH analogue, acetyl-Nle^4-c[Asp^5,D-Phe^7,Lys^{10}]α-MSH(4–10)-NH$_2$; NDP-MSH, [Nle^4,D-Phe^7]α-MSH; Omy, *Oncorhynchus mykiss* (rainbow trout); PCA, principal component analysis; Rno, *Rattus norvegicus* (Norway rat); RT-PCR, reverse transcription PCR; Sac, *Squalus acanthias* (spiny dogfish); SHU9119, cyclic MSH analogue, acetyl-Nle^4-c[Asp^5,D-Nal(2)^7,Lys^{10}]α-MSH (4–10)-NH$_2$; TM, transmembrane; Tru, *Takifugu rubripes* (Japanese pufferfish).

[1] To whom correspondence should be addressed (e-mail helgis@bmc.uu.se).

The nucleotide sequence data for rainbow trout MC4 and MC5 reported will appear in DDBJ, EMBL, GenBank® and GSDB Nucleotide Sequence Databases under the accession numbers AY534915 and AY534916 respectively.

serve as an important part of the central molecular regulation of food intake and growth in most vertebrates. However, much more information is needed to understand how this family of peptide-binding receptors, like many other such systems, has gained and possibly lost its functions during vertebrate evolution.

Fairly little is known about how 3D (three-dimensional) structures of GPCRs may be conserved through evolution. We have recently published a 3D model of the Hsa (*Homo sapiens*) MC4 receptor that may aid development of selective substances for this receptor [15]. During structural studies on this receptor, it was also shown that the MC4 receptor remarkably has a natural binding site for metal ions [15,16]. This has prompted speculations that endogenous zinc ions could participate in the regulation of MC receptor activity [16].

In the present paper, we report the cloning of two MC receptors in rainbow trout from a genomic library. We expressed the receptors in eukaryotic cells, characterized their pharmacological properties, including a test for metal-ion-binding sites, determined the anatomical distribution and performed the first comparative analysis of 3D models of GPCRs in non-mammalian species.

EXPERIMENTAL

Cloning and sequencing

Degenerate PCR primers were designed from sequence alignment of all known MC receptor sequences to match highly conserved domains of MC3, MC4 and MC5 receptor subtypes. The primer sequences were: 5′-TAYKTNACXATHTTYTRYGC-3′ and 5′-AANGCRAADATXARNGGRTG-3′ (X represents inosine or cytosine). Genomic DNA of rainbow trout was extracted from blood with a DNA isolation kit for blood (Boehringer Mannheim). Touch-down PCR was performed on rainbow trout genomic DNA using *Taq* DNA polymerase (Gibco) under the following conditions: initial denaturation for 5 min at 95 °C, followed by 12 cycles of 30 s at 95 °C, 45 s at 48–42 °C (lowered by 0.5 °C per cycle) and 1 min at 72 °C. This was continued by 35 cycles of 30 s at 95 °C, 45 s at 48 °C and 1 min at 72 °C, with a final extension of 5 min at 72 °C. Two different PCR products of desired length were isolated and cloned into the plasmid vector pCRII from TOPO cloning kit and transformed into TOP10 cells (Invitrogen) according to the manufacturer's instructions. The plasmid inserts were sequenced with vector-specific primers using ABI PRISM Big Dye Terminator Cycle Sequencing Ready Reaction Kit v2.0 and analysed by an automated ABI PRISM 310 or ABI PRISM 3100 fluorescent-dye sequencer (Applied Biosystems).

Isolation of full-length genes

Rainbow trout Lambda DASH® II Custom Genomic Library (Stratagene) was generously provided by Dr Pierre Rescan [INRA (Institut National de la Recherche Agronomique), Rennes, France]. The isolation of the genes was performed as described previously [17]. Briefly, the library was plated with the bacterial host strain. The plaques were lifted on to the nylon membranes (Osmonics), which were dried and hybridized with digested and ^{32}P-radiolabelled DNA probe. The filters were washed and exposed to autoradiographic film (Amersham Biosciences). Single clones were selected after the third screening, and DNA was isolated. A shotgun library was constructed and positive clones were selected by hybridization. The plasmid DNA was isolated and sequenced as described above.

Alignments and phylogenetic analysis

Alignment of predicted full-length amino acid sequences for the new genes, together with other known MC receptors, was made using CLUSTAL W 1.8 software [18]. The following receptor sequences (with their accession codes) were retrieved from GenBank® for this analysis: Hsa (*Homo sapiens*) MC1 (NM_002386), HsaMC2 (NM_000529), HsaMC3 (XM_009545), HsaMC4 (NM_005912), HsaMC5 (XM_008685), Mmu (*Mus musculus*) MC1 (NM_008559), MmuMC2 (NM_008560), MmuMC3 (NM_008561), MmuMC4 (NM_016977), MmuMC5 (NM_013596), Rno (*Rattus norvegicus*) MC2 (AAN64994), RnoMC3 (P32244), RnoMC4 (NP_037231), RnoMC5 (NP_037314), Gga (*Gallus gallus*) MC1 (D78272), GgaMC2 (AB009605), GgaMC3 (AB017137), GgaMC4 (AB012211), GgaMC5 (AB012868), Tru (*Takifugu rubripes*) MC1 (AAO65549), TruMC2 (AAO65550), TruMC4 (AAO65551), TruMC5 (AAO65552), Dre (*Danio rerio*) MC1 (NM_180970), DreMC2 (NM_180971), DreMC3 (NM_180972), DreMC4 (AY078989), DreMC5a (AY078990), DreMC5b (AY078991), Sac (*Squalus acanthius*) MC4 (AAO39833) and SacMC5 (J. Klovins, T. Haitina, A. Ringholm, M. Löwgren, D. Fridmans, M. Slaidina and H. B. Schiöth, unpublished work). The new genes have the following accession numbers: Omy (*Oncorhynchus mykiss*) MC4 (AY534915) and OmyMC5 (AY534916).

The alignment was bootstrapped 1000 times using SEQBOOT from the PHYLIP 3.6a3 package (http://evolution.gs.washington.edu/phylip.html) to obtain a total of 1000 different alignments. The obtained alignments were analysed with PROML from PHYLIP 3.6a3 using Jones–Taylor–Thornton model with 1000 bootstrap replicates and tree randomization per alignment, resulting in 1000 maximum likelihood trees. The consensus maximum likelihood tree was obtained with CONSENSE from PHYLIP 3.6a3 and plotted using TREEVIEW 1.6.6 (http://taxonomy.zoology.gla.ac.uk/rod/treeview.html).

3D modelling

The full-length amino acid sequences of the Omy (*Oncorhynchus mykiss*) MC4 and OmyMC5 receptors were aligned with the human orthologues and the bovine rhodopsin receptor using CLUSTAL W (1.82). The TM (transmembrane) region boundaries in the receptors were as follows. HsaMC4 receptor: TM1, Gln^{43}–Ile^{69}; TM2, Phe^{81}–Ile^{104}; TM3, Ile^{121}–Ile^{151}; TM4, Val^{163}–Ile^{187}; TM5, Ser^{190}–Met^{215}; TM6, Asn^{240}–Phe^{267}; TM7, Ser^{282}–Tyr^{302}; TM8, Gln^{307}–Ile^{317}. HsaMC5 receptor: TM1, Met^{36}–Ala^{62}; TM2, Pro^{70}–Leu^{99}; TM3, Ile^{114}–Ile^{144}; TM4, Ser^{159}–Leu^{179}; TM5, Tyr^{185}–Leu^{210}; TM6, Ser^{233}–Ser^{263}; TM7, Ser^{275}–Tyr^{295}; TM8, Gln^{300}–Ile^{310}. OmyMC4 receptor: TM1, Gln^{47}–Ile^{74}; TM2, Pro^{82}–Ile^{111}; TM3, Ser^{125}–Ile^{156}; TM4, Ala^{171}–Ile^{191}; TM5, Val^{198}–Met^{222}; TM6, Asn^{245}–Ser^{275}; TM7, Met^{286}–Tyr^{307}; TM8, Gln^{312}–Phe^{322}. OmyMC5 receptor: TM1, Gln^{45}–Ile^{72}; TM2, Pro^{80}–Leu^{109}; TM3, Gln^{123}–Ile^{154}; TM4, Ala^{164}–Met^{189}; TM5, Val^{196}–Met^{220}; TM6, Ser^{243}–Ser^{273}; TM7, Met^{284}–Tyr^{305}; TM8, Gln^{310}–Ile^{320}. Motifs common to GPCRs, such as the (E/D)RY motif in TM3 and the NPXXY motif in TM7 were checked to match precisely. The charges of the residues closest to the extracellular and cytosolic side of the α-helices were also taken into account when assigning the membrane-spanning regions. The structure of bovine rhodopsin was taken from crystallographic data [21] available on the Protein Data Bank (PDB 1HZX, chain A) and was loaded in Sybyl 6.4 software (Tripos, Germany) running on a MIPS R5000 workstation (Silicon Graphics O2®). The extracellular and cytosolic regions of the protein were deleted, as well as one subunit of the dimer. The distance and angle constraints were set between the residues closest to the cytosolic side.

A framework was constructed for the modelling. The co-ordinates from the rhodopsin structure were used as template when the amino acid residues were built with amino acids of the studied protein, each TM region was set as an ideal α-helix. The three substructures (amino acids) on the cytosolic side were not deleted for the TM regions, since constraints were defined in those regions. TM8 is not really a TM region, it is a postulated α-helix region located along the inner side of the plasma membrane. The amino acids in this region were introduced and then the region was set as an ideal α-helix. After this, the structure was suggested to be in a very strained state and subsequently refined. Charges ('KOLL_UNI') were loaded to the protein before minimization [vacuum; maximum iterations, 10 000; force-field, Tripos; termination, gradient 0.05 kCal/mol (1 kCal = 4.184 kJ); non-bonded cut-off, 8 Å (1 Å = 0.1 nm); di-electric function, distance; dielectric constant, 1; charges, use current; initial minimization, simplex] was carried out in subroutine 'Powell'.

PCA (principal component analysis)

PCA was performed using SIMCA-P+ 10.0 software (Umetrics AB, Umeå, Sweden) [22]. Distances between key amino acids in the receptors (especially well-preserved amino acids), one from each of the seven TM helices, were measured. The distances were as follows. Hsa MC4 receptor: Asp^{126} (TM3) to Asn^{62} (TM1), Ile^{104} (TM2), Trp^{174} (TM4), His^{214} (TM5), Pro^{260} (TM6) and Asp^{298} (TM7), and Ile^{104} to Asn^{62}, Trp^{174}, His^{214}, Pro^{260} and Asp^{298}. Hsa MC5 receptor: Asp^{119} to Asn^{54}, Ile^{96}, Trp^{167}, His^{207}, Pro^{253} and Asp^{291}, and Ile^{96} to Asn^{54}, Trp^{167}, His^{207}, Pro^{253} and Asp^{291}. OmyMC4 receptor: Asp^{131} to Asn^{66}, Ile^{108}, Trp^{179}, His^{219}, Pro^{265} and Asp^{303}, and Ile^{108} to Asn^{66}, Trp^{179}, His^{219}, Pro^{265} and Asp^{303}. OmyMC5 receptor: Asp^{129} to Asn^{64}, Ile^{106}, Trp^{177}, His^{217}, Pro^{263} and Asp^{301}, and Ile^{106} to Asn^{64}, Trp^{177}, His^{217}, Pro^{263} and Asp^{301}. PCA was performed on this data matrix. Different GPCRs served as observations and the distances as variables for each GPCR. The data were not modified and variables were not comprised in order to get better goodness of fit (R2) and predicted variation (Q2).

Cloning into pCEP expression vector

Full-length coding sequences were amplified by means of PCR from receptor genes containing pUC18 plasmids with *Pfu* polymerase (Fermentas) using *Hin*dIII and *Xho*I restriction sites containing primers for the N- and C-terminus respectively. Obtained fragments were then digested with both restriction enzymes and gel-purified before ligation into a modified pCEP expression vector [23]. All constructs were sequenced.

Expression of receptors

HEK-293 (human embryonic kidney) cells, grown to 50–70 % confluence, were transfected with 10 μg of the construct using FuGENE 6 Transfection Reagent (Roche) according to the manufacturer's instruction. The cells were grown in Dulbecco's modified Eagle's medium/F-12 nutrient mixture (1:1) with GlutaMAX I containing 10 % foetal bovine serum, 100 units/ml penicillin, 100 μg/ml streptomycin, 2.5 μg/ml amphotericin B, and 250 μg/ml geneticin G-418 (Gibco); in a humidified atmosphere containing 5 % CO_2 at 37 °C. Semi-stable cell lines, expressing target receptor, were obtained by selecting for growth in the presence of 100 μg/ml hygromycin B (Invitrogen), first added 24 h after transfection.

Radioligand-binding assay

Radioligand-binding experiments were performed as described previously [12]. Briefly, HEK-293 cells expressing rainbow trout receptors were harvested, and cell membranes were isolated. The binding was performed in a final volume of 100 μl for 3 h at room temperature (18–20 °C). Saturation experiments were carried out with serial dilutions of ^{125}I-labelled NDP-MSH {[Nle^4, D-Phe^7]α-MSH (melanocyte-stimulating hormone)} and 1 μM unlabelled NDP-MSH. Competition experiments were performed with constant 0.6 nM concentration of ^{125}I-labelled NDP-MSH and serial dilutions of competing unlabelled ligands: NDP-MSH, α-MSH, β-MSH, γ_1-MSH, ACTH (adrenocorticotropic hormone) (1–24), MTII {acetyl-Nle^4-c[Asp^5,D-Phe^7,Lys^{10}]α-MSH(4–10)-NH_2}, HS024 {c[acetyl-Cys^3,Nle^4,Arg^5,D-Nal^7, Cys-$NH_2{}^{11}$]α-MSH-(3–11)} and SHU9119 {acetyl-Nle^4-c[Asp^5, D-Nal(2)^7,Lys^{10}]α-MSH (4–10)-NH_2} (Neosystem). The membranes were collected by filtration on glass fibre filters (PerkinElmer), washed and dried. Solid scintillator sheets (PerkinElmer) were melted on dried filters and radioactivity was counted with automatic Microbeta counter 1450 (Wallac). Binding assays were performed in duplicate from at least three independent experiments. Non-transfected cells did not show any specific binding with ^{125}I-labelled NDP-MSH. The results were analysed with Prism 3.0 software package (GraphPad).

Radioligand competition binding assay with zinc

The competition binding assay was performed as described above, but all reaction components were resuspended in the buffer containing 137 mM NaCl, 5 mM KCl, 0.44 mM KH_2PO_4, 4.2 mM $NaHCO_3$, 1.2 mM $MgCl_2 \cdot 6H_2O$ and 20 mM Hepes, pH adjusted to 7.4. Competition experiments were performed with constant 0.6 nM concentration of ^{125}I-labelled NDP-MSH and various concentrations of $ZnCl_2$ (Sigma).

cAMP assay

This assay was performed as described previously [12]. Briefly, cells expressing rainbow trout receptors were incubated with 2.5 μCi/ml of [^{3}H]ATP, before collection and resuspension in buffer containing 137 nM NaCl, 5 mM KCl, 0.44 mM KH_2PO_4, 4.2 mM $NaHCO_3$, 1.2 mM $MgCl_2 \cdot 6H_2O$, 20 mM Hepes, 1 mM $CaCl_2$, 10 mM glucose and 0.5 mM isobutylmethylxanthine, pH 7.4. The stimulation reaction was performed with approx. 2×10^5 cells and various concentrations of MTII and SHU9119 alone, or with a fixed concentration (0.1 μM) of SHU9119. After incubation, cells were centrifuged at 900 ***g*** and lysed. ATP/ADP and cAMP from cell contents were separated using chromatography columns, with an internal standard of 0.5 nCi/ml of [^{14}C]cAMP used, scintillation cocktail added and samples counted using a Tri-carb liquid scintillation β-counter. After standardization of results the amounts of [^{3}H]cAMP converted from [^{3}H]ATP and EC_{50} values were calculated. All experiments were performed in duplicate and repeated three times.

RT-PCR (reverse transcription PCR) and hybridization analysis

The total RNA was isolated from number of peripheral tissues (head kidney, liver, adipose tissue, ovary, pyloric caecum, intestine and muscle) and several brain regions (telencephalon, hypothalamus, optic tectum, cerebellum and brain stem) [17]. Tissues were rapidly dissected from freshly killed rainbow trout within 5 min and stored in RNAlater (Ambion) for 24–72 h at

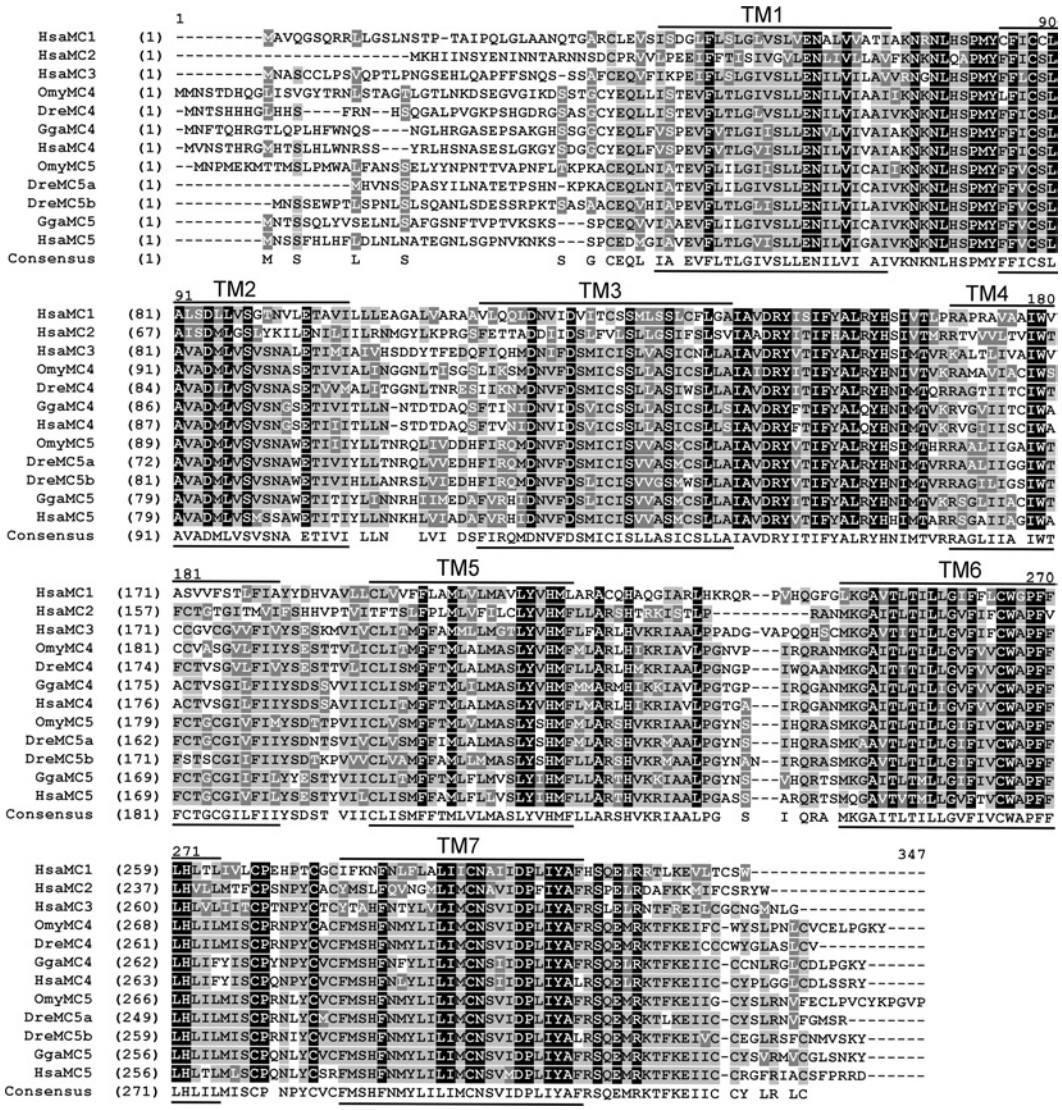

Figure 1 Amino acid sequence alignment of MC receptors constructed using CLUSTAL W 1.8

Putative TM regions are marked with lines. Black boxes mark conserved amino acid positions. Accession numbers are listed in the Experimental section.

4 °C before RNA extraction. Total RNA and then cDNA was prepared as described by Larson et al. [17]. The cDNA obtained was used as a template for PCR with specific primers for the receptor genes: for the MC4 receptor gene (expected size 395 bp), 5′-GGCGTGCTCTTCATTATCTAC-3′ and 5′-GTCTTCCTCATCTCTTGGCTC-3′; and for the MC5 receptor gene (expected size 399 bp), 5′-GGCGTCTATGTGTTCTCTCCT-3′ and 5′-AGGATAAGGTGGAGGAAGAAG-3′. The PCR products were analysed and hybridization was performed as described previously [12]. Briefly, DNA from the gel was transferred on to nylon filters and hybridized with a random-primed ^{32}P-labelled, receptor-specific probe. After hybridization, filters were washed and exposed to autoradiography film. Due to the appearance of double bands (results not shown), the PCR products were denatured in 3 % formaldehyde/25 % formamide solution and separated on a 1.4 % agarose gel using Mops buffer (20 mM Mops, 2 mM sodium acetate and 1 mM EDTA), resulting in a single band. The PCR products obtained from the genomic DNA were used as positive controls in the hybridization blots. Sequence analysis of the PCR products confirmed the presence of target receptor sequences. The RT-PCR reactions and hybridization were performed three times each.

RESULTS

Cloning and sequence analysis

The degenerate PCR resulted in products with an expected size of 450 bp. The following cloning and sequencing of the fragments allowed us to identify two different clones with high similarity to MC4 and MC5 receptors respectively. The clones were used for high-stringency screening of a rainbow trout genomic library. Two positive clones were isolated and sequenced; as a result, two different genes of 1017 bp and 1023 bp were identified, corresponding to putative MC receptors of 339 and 341 amino acids respectively. The amino acid sequence alignment of the new rainbow trout genes together with human, chicken and zebrafish MC receptors is shown in Figure 1. The percentage similarities of amino acid sequences are shown in Table 1. The rainbow trout receptor of 339 amino acids had the highest identity with the

Table 1 Percentage identity of the full-length amino acid sequences for the MC receptor subtypes from different species

GenBank® accession numbers are listed in the Experimental section.

	HsaMC1	HsaMC2	HsaMC3	SacMC4	DreMC4	Tru MC4	OmyMC4	GgaMC4	RnoMC4	MmuMC4	HsaMC4	SacMC5	DreMC5a	DreMC5b	TruMC5	OmyMC5	GgaMC5	RnoMC5	MmuMC5	HsaMC5
HsaMC1	100	41	48	47	48	50	46	46	46	46	46	49	46	44	44	42	46	46	46	45
HsaMC2		100	45	44	46	48	44	45	44	45	44	48	47	44	43	42	47	46	45	45
HsaMC3			100	61	61	62	58	56	56	56	56	61	60	59	57	55	61	58	58	59
SacMC4				100	76	74	75	70	72	71	73	67	67	65	66	64	68	64	64	65
DreMC4					100	79	75	69	70	69	69	66	67	64	64	63	66	63	63	62
Tru MC4						100	77	68	68	68	67	66	65	63	64	62	65	62	62	61
OmyMC4							100	69	70	69	69	66	65	63	66	64	64	62	61	60
GgaMC4								100	87	86	88	65	62	62	62	60	64	61	60	60
RnoMC4									100	98	93	64	60	62	61	59	62	61	60	61
MmuMC4										100	94	63	61	62	61	59	62	61	61	61
HsaMC4											100	64	61	63	61	59	64	61	60	61
SacMC5												100	75	71	72	72	78	73	73	72
DreMC5a													100	74	79	82	74	69	69	70
DreMC5b														100	74	70	71	70	70	67
TruMC5															100	79	72	68	68	69
OmyMC5																100	72	67	67	66
GgaMC5																	100	80	80	79
RnoMC5																		100	95	82
MmuMC5																			100	82
HsaMC5																				100

MC4 receptors, with 69 % (human) to 77 % (zebrafish) amino acid identity and was therefore designated as the OmyMC4 receptor. The other rainbow trout receptor showed the highest identity with the DreMC5a receptor (82 %) and was named the OmyMC5 receptor. The similarity between the two new rainbow trout receptors is 64 %.

Phylogenetic analysis

Phylogenetic analysis was performed using the maximum likelihood method. The topology of the tree was the same with (results not shown) or without an out-group (Figure 2). The OmyMC4 receptor grouped with the DreMC4 receptor, corroborating the identification above based on the percentage identity. The OmyMC5 receptor branched together with DreMC5a receptor, while the DreMC5b receptor probably rose in an earlier teleost duplication.

3D structure modelling

In order to gain insight into the evolution of the 3D structures of the MC receptors we performed molecular modelling on the Omy and Hsa MC4 and MC5 receptors. The framework for the models was generated from the co-ordinates of bovine rhodopsin. No mutagenesis data from MC receptors were taken into account during the modelling. The four receptors were modelled and the results are presented in Figure 3. The resulting minimization energy for all the four receptors was similar, ranging from approx. 3600 to 4500 kCal/mol.

The modelled HsaMC4 receptor gave the energy of 3646 kCal/mol. Asp^{126}, Ile^{125}, Asp^{126}, Ile^{129}, Ser^{132} and Leu^{133} in TM3, Ile^{104} in TM2 and Asp^{298} in TM7 are facing the space between TM2, TM3 and TM7. Trp^{174} in TM4 was pointing towards the extracellular side, whereas Pro^{260} in TM6 is facing the lipid membrane. His^{214} in TM5 and Asn^{62} in TM1 are both facing to the centre of the receptor. The HsaMC5 receptor had the energy of 4425 kCal/mol. Asp^{119} in TM3 is pointing towards His^{207} of TM5. Ile^{96} in TM2 and Asp^{291} in TM7 are facing into the receptor. Pro^{253} in TM6 and Asn^{54} of TM1 are facing the lipid membrane, whereas Trp^{167} in TM4 is facing the cytosolic side of the membrane. Compared with

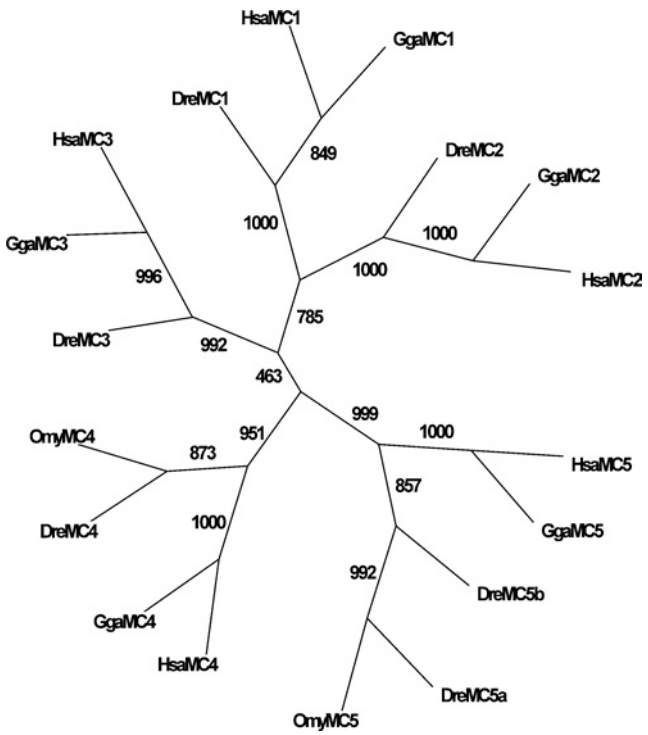

Figure 2 Phylogenetic analysis of MC receptors using full-length amino acid sequences

The consensus tree was generated by maximum likelihood analysis (PHYLIP 3.6a3). The numbers above the nodes indicate bootstrap replicates. Accession numbers are listed in the Experimental section.

their counterparts in the HsaMC4 receptor, TM1 and TM4 have both rotated almost 180° around their own axis in the HsaMC5 receptor. TM3 has rotated approx. 90° clockwise compared with that of the HsaMC4 receptor. The OmyMC4 receptor had the energy of 4481 kCal/mol. Asp^{131} in TM3 is facing TM6, whereas Asp^{303} in TM7 is pointing towards Ile^{108} in TM2. Asn^{66} in TM1,

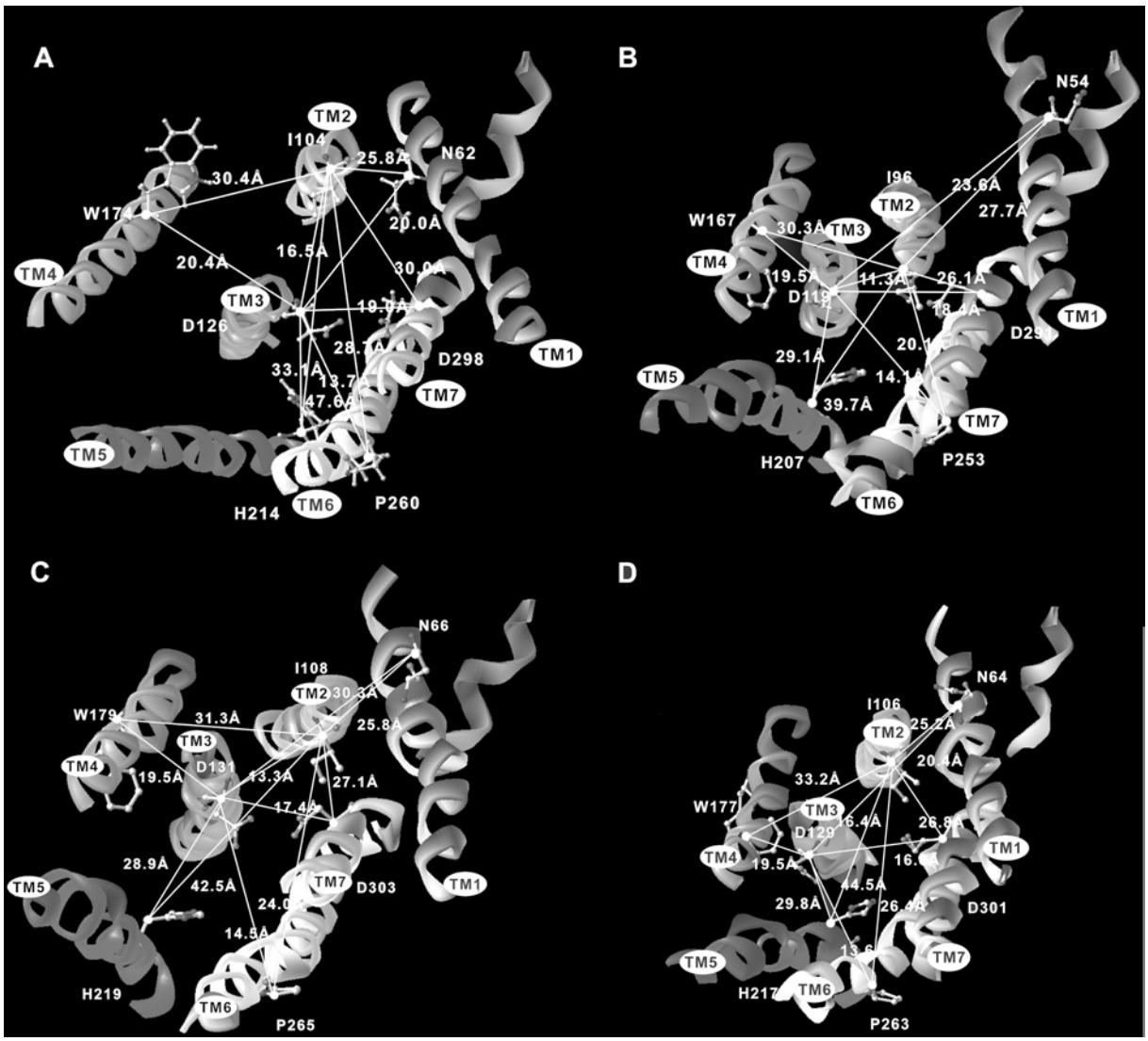

Figure 3 Orientation of TM1–TM7 regions in the computer model, based on the crystallized bovine rhodopsin receptor

The models are seen from the extracellular side: (**A**) HsaMC4 receptor, (**B**) HsaMC5 receptor, (**C**) OmyMC4 receptor, (**D**) OmyMC5 receptor. Positions and directions of highly conserved amino acid residues are highlighted. Distances between these amino acids are noted.

Table 2 Distances between TM regions in Hsa and Omy MC4 and MC5 receptors used for PCA

	Distance (Å)										
GPCR	TM2–TM1	TM2–TM3	TM2–TM4	TM2–TM5	TM2–TM6	TM2–TM7	TM3–TM1	TM3–TM4	TM3–TM5	TM3–TM6	TM3–TM7
HsaMC4R	25.8	16.48	30.38	47.55	28.72	30.01	19.95	20.41	33.07	13.72	18.97
HsaMC5R	27.65	11.32	30.29	39.65	20.14	26.05	23.6	19.51	29.10	14.08	18.38
OmyMC4R	25.76	13.26	31.26	42.52	24.03	27.06	20.3	19.51	29.76	14.48	17.4
OmyMC5R	25.18	16.4	33.23	44.53	26.38	26.75	20.35	19.49	29.78	13.57	16.64

Pro[265] in TM6 and Trp[179] in TM4 are all facing the lipid membrane. His[219] in TM5 is facing the interior of the receptor. TM3 has only rotated approx. 45° compared with the HsaMC4 receptor. The OmyMC5 receptor gave the energy of 3854 kCal/mol. Asp[129] in TM3 is pointing towards TM5 and His[217] in TM5 is facing the intrareceptor space. Trp[177] in TM4 is pointing towards the cytosolic side of the membrane, whereas Pro[263] in TM6 and Asn[64] of TM1 are facing the lipid membrane. Asp[301] in TM7 and Ile[106] in TM2 are facing into the space between TM1, TM2, TM3 and TM7. TM1, TM3 and TM4 are rotated in the same fashion as in the HsaMC5 receptor.

PCA of 3D structure

PCA on distances between the TM regions within each receptor (Table 2) shows that the rainbow trout receptors have a closer structural similarity between themselves than do the human receptors. Figure 4 shows the loading plot of distances. The

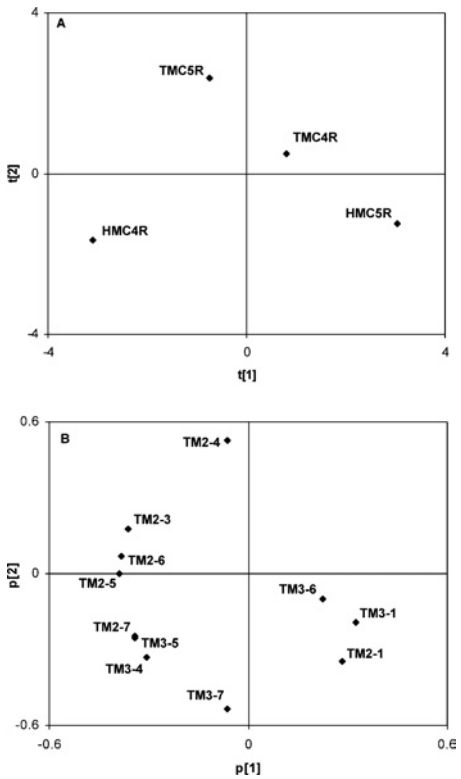

Figure 4 PCA of distances within the four modelled receptors: HsaMC4 receptor, HsaMC5 receptor, OmyMC4 receptor and OmyMC5 receptor

(**A**) Score plot of the modelled GPCRs. The two first principal component score vectors, t[1] and t[2], are plotted. The principal component score vectors are linear combinations of the distances and the score plot is a summary of the relationships between the GPCRs. (**B**) Loading plot of the distances in the receptors. Plot of the first two loading vectors, p[1] and p[2]. The loading vectors are the weights combining the original variables (distances) to form the score vectors. The loading plot shows the relationships between the variables and is a means to interpret the scoring plot. The two plots are complementary and a direction in one plot corresponds to the same direction in the other plot.

HsaMC4 receptor is the only receptor located in the lower-left quadrant of the scoring plot (Figure 4A), while in the loading plot, both the distances to TM7 are located in that same quadrant (Figure 4B). It seems evident that it is the distances from TM7 to TM2 and TM3 that have diverged the most. This divergence is not seen in any mutagenesis data, but is entirely an effect from the energy minimization of the model. The result of the modelling also indicates that TM4 and TM5 may be more distant to the other regions in HsaMC4 receptor than in any of the other models (Figure 3). TM4 and TM5 have, however, low identity with bovine rhodopsin, and the rhodopsin model therefore does not serve as a good template for this region. Moreover, there are not so many mutagenesis experiments performed in these regions that could help to clarify their importance. The HsaMC5 receptor is in the lower-right quadrant of the score plot (Figure 4A) that coincides with the distance between TM1 and TM2 in the loading plot (Figure 4B). Taken together, the HsaMC4 receptor thus seems to have diverged differently as compared with the HsaMC5 receptor (Figure 3 and Table 2). The rainbow trout receptors are closest to each other on the scoring plot. They are both together in the upper half of the scoring plot, which is related to the distances between TM2 and TM3, and between TM2 and TM4, that are also found in the top-left quadrant of the loading plot. Looking at Table 2, we can see that the differences between the receptors are mainly related to the distance between TM2 and TM3 and less related to the distances between TM2 and TM4. Considering the overall distances in all four receptors, TM5 and TM6 do not seem to contribute to the structural difference between the receptors that are found in the scoring plot. Thus the models indicate that TM1, TM2, TM3 and TM7 are most responsible for the structural divergence of the different MC receptors (Figure 3).

Competition binding

In order to characterize the new rainbow trout receptors pharmacologically, the synthesized human peptides were used as ligands in a binding assay. α-MSH is fully conserved between human and rainbow trout, whereas there are minor differences in the sequence of β-MSH and ACTH, but not within the predicted core binding region of the peptides. Figure 5 shows saturation and competition curves for the OmyMC4 and OmyMC5 receptors. Table 3 shows the K_d and K_i values obtained from saturation and competition experiments respectively. For comparison, Table 3 also includes previously published results for the human MC receptors tested with the same methodological approach. The OmyMC4 and OmyMC5 receptors bind NDP-MSH with similar affinities, which are slightly higher (approx. 3-fold) than for the human orthologues. Likewise, the endogenous ligand α-MSH had 3.2-fold higher affinity, whereas β-MSH had a very similar affinity for the OmyMC4 receptors, compared with the HsaMC4 receptor. Interestingly, another natural ligand γ_1-MSH had 112-fold higher affinity for the OmyMC4 receptor as compared with the same receptor subtype in human. ACTH (1–24), which is generally considered to be equipotent to full-length ACTH (1–39), had also clearly higher affinity (36-fold) for the OmyMC4 receptor, as compared with HsaMC4 receptor. On the other hand, the synthetic ligands MTII and HS024 had 4.8- and 8.8-fold lower affinities respectively for OmyMC4 receptor, whereas the same receptor binds another synthetic ligand, SHU9119, with 61.8 pM affinity, that is 11-fold higher than as for the HsaMC4 receptor. The OmyMC5 receptor binds the endogenous ligands with clearly higher affinities than the HsaMC5 receptor, whereas the affinities for the synthetic ligands are lower. So, α-MSH had 83-fold, β-MSH had 120-fold, γ_1-MSH had 79-fold and ACTH (1–24) had almost 106-fold higher potency, whereas MTII had slightly lower, HS024 had 10-fold and SHU9119 had 18-fold lower affinities for the OmyMC5 receptor. Overall, however, the characteristic potency order NDP-MSH > α-MSH > β-MSH > γ_1-MSH determined for the HsaMC5 receptor [24] was conserved for the OmyMC5 receptor.

Identification of zinc-binding site

OmyMC4 and OmyMC5 receptors expressed in HEK-293 cells were tested in competition binding for their ability to bind zinc. Binding curves are shown in Figure 6. The analysis of the curves (Table 3) showed that the OmyMC4 receptor has a zinc-binding site with a K_i of $0.481 \pm 0.016\ \mu$M, which is approx. 40-fold higher compared with the K_i of $20.07 \pm 1.33\ \mu$M for the HsaMC4 receptor. In contrast, the OmyMC5 receptor does not bind zinc.

Measurement of intracellular cAMP

The expressed rainbow trout MC receptors were also tested for their ability to couple to G-proteins and induce the accumulation of cAMP, as well as for the agonistic–antagonistic relationship between synthetic substances. Both receptor subtypes reached maximal levels of response when stimulated with agonists. As shown in Figure 7, SHU9119 had no effect on intracellular cAMP

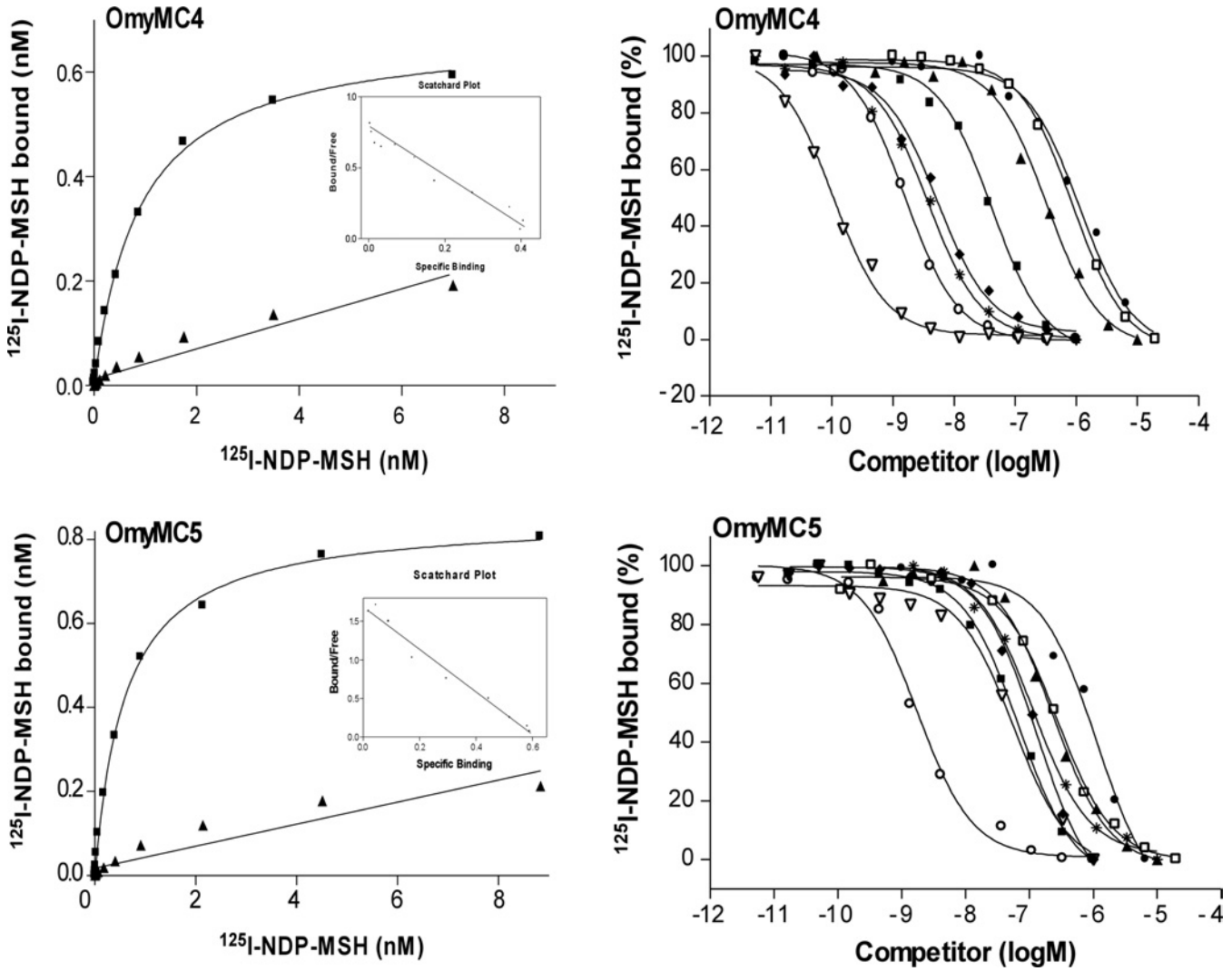

Figure 5 Saturation curves with Scatchard plots and competition curves for the OmyMC4 and OmyMC5 receptors expressed in HEK-293 cells

The saturation curves (left) were obtained with ^{125}I-labelled NDP-MSH and the figure shows total binding (filled square) and binding in the presence of 2 μM unlabelled NDP-MSH (filled triangle). The lines represent the computer-modelled best fit of the data assuming that ligands are bound to one site. The competition curves (right) for NDP-MSH (open circle), α-MSH (filled triangle), β-MSH (open square), γ_1-MSH (filled circle), ACTH (filled square), MTII (asterisk), HS024 (filled rhombus) and SHU9119 (open triangle) were obtained by using a fixed concentration of approx. 0.6 nM ^{125}I-labelled NDP-MSH and varying concentrations of the unlabelled competing peptide.

Table 3 K_d and K_i values (means ± S.E.M.) obtained from saturation and competition curves respectively for MC peptide analogues and Zn^{2+} on the Omy and Hsa MC4 and MC5 receptors

	K_d or K_i value (nmol · l^{-1})			
Ligand Receptor...	OmyMC4	HsaMC4*	OmyMC5	HsaMC5‡
[^{125}I]NDP-MSH (K_d)	0.693 ± 0.099	1.78 ± 0.36	0.454 ± 0.038	5.05 ± 1.00
NDP-MSH (K_i)	0.541 ± 0.113	1.96 ± 0.39	0.730 ± 0.056	2.39 ± 0.10
α-MSH (K_i)	162 ± 48	522 ± 122	98.6 ± 29.7	8240 ± 1670
β-MSH (K_i)	342 ± 99	387 ± 208	120 ± 8	14 400 ± 1670
γ_1-MSH (K_i)	461 ± 88	51 800 ± 12 000	538 ± 46	42 600 ± 6600
ACTH (1–24) (K_i)	20.8 ± 0.5	755 ± 151	26.1 ± 1.4	2760 ± 780‖
MT II (K_i)	1.38 ± 0.46	6.60 ± 0.82†	30.4 ± 13.7	46.1 ± 7.9†
HS024 (K_i)	3.00 ± 0.87	0.341 ± 0.089	35.1 ± 10.5	3.29 ± 1.15§
SHU9119 (K_i)	0.0618 ± 0.0146	0.689 ± 0.251	20.9 ± 5.6	1.12 ± 0.31†
$ZnCl_2$ (K_i)	481 ± 16	20 070 ± 1330¶	NB	ND

Data taken from *[31], †[32], ‡[33], §[10], ‖[34], ¶[15]. ND = not determined; NB = no binding detected.

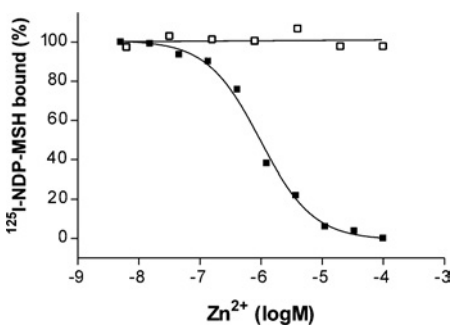

Figure 6 Competition curves for the OmyMC4 (filled square) and OmyMC5 (open square) receptors expressed in HEK-293 cells, obtained by using a fixed concentration of approx. 0.6 nM ^{125}I-labelled NDP-MSH and varying concentrations of $ZnCl_2$

accumulation in the cells expressing the OmyMC4 receptors at any dose tested. In contrast, MTII induced a dose-dependent cAMP accumulation with an EC_{50} of 0.582 nM for the OmyMC4

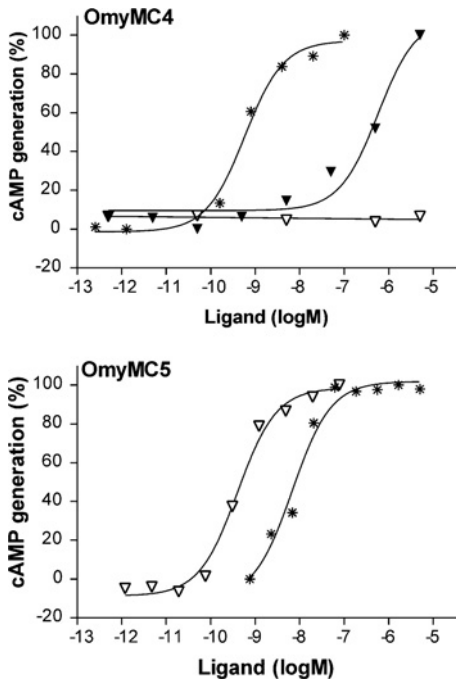

Figure 7 Generation of cAMP in response to MTII (asterisk), MTII with a fixed concentration of 0.1 μM SHU9119 (filled triangle) and SHU9119 (open triangle) for the OmyMC4 and OmyMC5 receptors expressed in HEK-293 cells

Untransfected cells showed no adenylate cyclase activity in response to MTII and SHU9119 (results not shown). The cAMP assay was performed in duplicate and was repeated three times for each receptor subtype.

receptor. When the cells were incubated with increasing concentrations of MTII and a fixed concentration of SHU9119, the EC_{50} was shifted to 522 nM for the OmyMC4 receptor, indicating an inhibition of the cAMP accumulation that would have been expected for a functional antagonist. For the cells expressing the OmyMC5 receptors, however, we obtained dose-dependent increase in cAMP accumulation by both MTII and SHU9119 with EC_{50} values of 6.86 nM and 0.404 nM respectively, reaching the same maximum levels, which indicates full agonistic properties of these ligands on the OmyMC5 receptor.

Tissue distribution

The tissue distribution of the rainbow trout MC receptor mRNA was determined by RT-PCR. The results of the RT-PCR for each of the receptor gene are shown in Figure 8. Each pair of PCR primers was designed to be specific for one receptor subtype. No cross-hybridization was detected in our samples. It should be noted that the PCR assay was not designed for quantification, but gives good qualitative information. The OmyMC4 receptor did not show strong signals in any type of tissue analysed. Among the peripheral tissues, the expression was detected only in head kidney, while in CNS (central nervous system), it was detected in three brain regions: telencephalon, optic tectum and the highest levels in the hypothalamus. The OmyMC5 receptor showed very high signals in two peripheral tissues: head kidney and ovary, while the signal in pyloric caecum was very weak and could not be detected with ethidium bromide staining. All analysed brain regions showed expression of the OmyMC5 receptor, with the strongest signal in telencephalon, followed by slightly weaker signals in hypothalamus, weaker signals still in the optic tectum and cerebellum, and a very weak signal, detectable only on the Southern blot, in the brain stem.

DISCUSSION

We have shown the presence of both MC4 and MC5 receptors in rainbow trout. This is in agreement with our findings in Japanese pufferfish (*Takifugu rubripes*), which has four of the mammalian MC receptor subtypes, including the MC4 and MC5 receptors. Japanese pufferfish, however, lacks an MC3 receptor. Zebrafish has one MC4 receptor, but also two copies of the MC5 receptor. The OmyMC5 receptor is most similar to the DreMC5a receptor (82 % amino acid identity), whereas it has clearly less similarity to the DreMC5b receptor (75 % identity). The additional copy of the MC5 receptor in zebrafish is likely to have occurred through an independent tetraploidization event that teleost fishes underwent, before the split of rainbow trout and zebrafish [25,26]. Our screening of a rainbow trout genomic library, that was similar to the one performed on zebrafish (resulting in two copies), did not provide any evidence for additional copies, suggesting that a putative MC5b receptor copy in rainbow trout may have been lost.

We also investigated the 3D structure of the receptors and their divergence through molecular modelling. Interestingly, the PCA analysis on the distance matrices (Figure 4) indicates that the OmyMC4 and OmyMC5 receptors are the most similar of the four receptors. It is also intriguing that the models indicate that the human receptors have diverged in different regions within the receptor protein. The relative position of TM7 has diverged most for the HsaMC4 receptor and OmyMC4 receptor, whereas the relative positions of TM1 and TM2 may have diverged most in the HsaMC5 and OmyMC5 receptors. It also appears that the 3D structure of the two human receptors has diverged differently. We recently published a detailed model of the HsaMC4 receptor, supported by artificial metal-ion-binding sites that provided specific information about the orientation of the TM2 and TM3 regions [15]. The binding pocket of the MC4 receptor is suggested to be located between TM2, TM3 and TM7 according to this model. The HsaMC4, HsaMC5, OmyMC4 and OmyMC5 receptor models show overall similarities with the HsaMC4 receptor model published by Lagerström et al. [15], with regard to the position of TM2 and TM3, whereas the main differences are related to TM7. We are not aware of any previous evolutionary comparative 3D modelling performed on GPCRs. We believe that our models will provide important guidance in the differences between these two subtypes.

The OmyMC4 receptor has similar affinity for α-MSH and β-MSH, whereas it has much higher (36-fold) affinity for ACTH as compared with the HsaMC4 receptor. This is very interesting in light of our findings in Japanese pufferfish and chicken showing that the MC4 receptor has higher affinity for ACTH-derived peptides as compared with α- and β-MSH [12]. Moreover, the MC1 and MC5 receptor in Japanese pufferfish and chicken have also higher affinity for ACTH-derived peptides as compared with α-, β- and γ-MSH. The OmyMC5 receptor also has much higher, or more than 100-fold higher affinity for ACTH as compared with the HsaMC5 receptor. Taken together, it is tempting to speculate that ACTH-derived peptides may have played an important role as the 'original' ligand at the MC receptors, while the specificity of the different subtypes for the α-, β- and γ-MSH peptides may have appeared at later stages during vertebrate evolution.

The mammalian MC5 receptor has the same potency order for binding to the different MC peptides as the MC1 receptor, although it binds to all these ligands with much lower affinity.

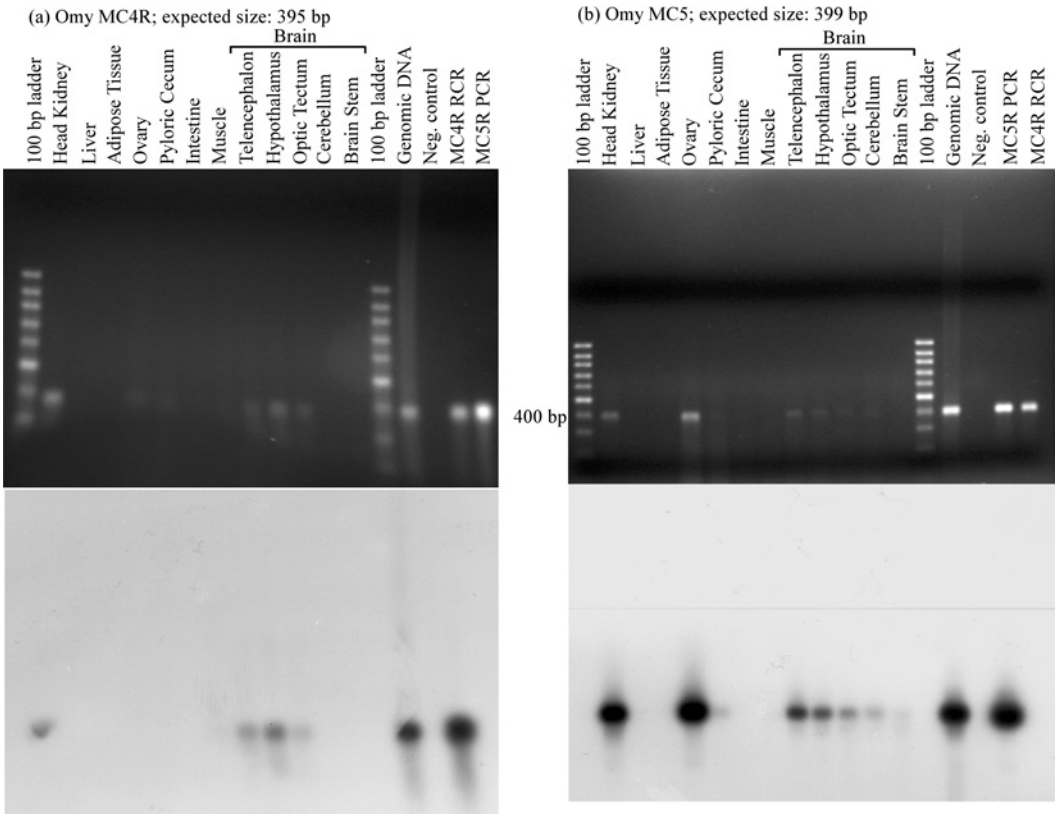

Figure 8 Expression of OmyMC4 (a) and OmyMC5 (b) receptor mRNA as determined by RT-PCR

The tissues, controls and expected sizes of the PCR products are denoted above each gel. Ethidium-bromide-stained agarose gels are presented above autoradiographs of Southern blots, hybridized with gene specific probes. PCR and hybridization were performed three times with qualitatively similar results.

The low affinity of this receptor has even prompted speculations that the MSH peptides may not be the natural ligands for this subtype in humans. Our results show that the OmyMC5 receptor has much higher affinity for all of the endogenous peptides as compared with the human orthologue. This indicates that, at least in fish and, perhaps, also during early vertebrate evolution, MSH peptides were important for this receptor.

We also determined the binding of several synthetic peptides to the rainbow trout receptors. The cyclic MSH analogues, MTII, SHU9119 and HS024, are peptides that are widely used for *in vivo* studies. These show clear preference for the OmyMC4 receptor above the OmyMC5 receptor. The potencies of these substances are high or very high, which makes them all very suitable for physiological studies in rainbow trout. Moreover, we showed that SHU9119 acts as a full antagonist and that MTII acts as a full agonist at the OmyMC4 receptor in second messenger studies. This means that if the MC4 receptor plays a similar role in rainbow trout as in mammals, the administration of SHU9119 should increase food intake, whereas administration of MTII should decrease food intake. Our preliminary data on injection of these substances into rainbow trout also indicate that this is the case (E. T. Larson, J. Schjolden, H. B. Schiöth and S. Winberg, unpublished work), supporting further a conserved agreement between the pharmacology and physiology of the MC4 receptors through vertebrate evolution [14].

In light of the recent interesting findings that MC receptors may have binding sites for zinc [15,16], we tested if zinc could also bind these 'ancient' MC receptors. Remarkably, we found that the OmyMC4 receptor has a relatively high-affinity binding site for zinc. It seems evident that there exists an evolutionarily conserved ability to bind this metal ion. Holst et al. [16] reported that zinc bound to the HsaMC4 receptor with a K_i of 19 μM, which is in line with what we have found (results not shown) and previously reported (K_i of 20 μM; [15]). Interestingly, the affinity of zinc for the OmyMC4 receptor was considerably higher (K_i of 0.5 μM). The zinc ion works in an antagonistic fashion at the OmyMC4 receptor, which is in agreement with what we found for the HsaMC4 receptor, whereas Holst et al. [16] found zinc caused small partial stimulation of the HsaMC4 receptor. The differences are probably related to differences in the experimental conditions [15]. It is tempting to speculate that endogenous zinc ions could be a factor in the regulation of MC receptor activity [16], considering that zinc, after iron, is the most abundant transition metal in the brain [27]. Most of the zinc is, however, incorporated into metal–protein complexes. The high affinity of the OmyMC4 receptor makes a role of endogenous zinc even more likely. This would be possible particularly in the CNS, where zinc is found stored in synaptic vesicles and can be co-released with the neurotransmitter to reach concentrations of up to 300 μM in the synaptic cleft [28]. Moreover, vesicular zinc is also found in the hypothalamus [29], the main expression site for the MC4 receptor. Rather surprisingly, the OmyMC5 receptor did not bind the metal ion, and our studies on the HsaMC5 receptors indicate the same. Previously, it was shown that the HsaMC1 receptor also binds zinc in similar fashion as the HsaMC4 receptor [16]. It has been difficult to determine the location of this binding site within the receptor protein. Mutagenesis studies indicate that Cys^{271} in extracellular loop 3 of the MmuMC1 receptor could be involved. This residue is conserved in the HsaMC1 receptor, and the HsaMC4 and OmyMC4 receptors, as well as in the OmyMC5

and HsaMC5 receptors. It is possible that the metal ion binds in a bidentate or perhaps even a tridentate metal-ion site [16]. It has been speculated that the Asp^{119} in the MmuMC1 receptor, a residue that is conserved in all MC receptor sequences found so far, could also participate in this binding site. Our models of the MC4 and MC5 receptors (see Figure 3) indicate that this could be the case as this residue is turned towards the binding cavity. Looking at the sequence differences between the MC4 and MC5 receptors and possible explanations for why the OmyMC5 receptor does not bind zinc, we found that this could be related to the fact that the OmyMC5 and HsaMC5 receptors lack one of the proline residues (replaced by Leu^{278} in the OmyMC5 receptor) in between Cys^{274} and Cys^{280}, in the third extracellular loop, that may be part of the interaction point with zinc. Proline is known to form kinks within TM regions and this proline residue may be crucial in causing conformational rigidity enabling the zinc to interact with one or the other cysteine residues.

RT-PCR is not well suited for quantitative analysis of gene expression, but it is very effective to detect the expression of genes in wide range of tissues. The mammalian MC4 receptor is only expressed in the brain. The OmyMC4 receptor was found in the hypothalamus and telencephalon. Somewhat surprisingly, the receptor was also found in one peripheral tissue, the head kidney. It is interesting that in chicken, the MC4 receptor is expressed in a wide variety of peripheral tissues, including the heart, adrenal glands, ovaries, testes, spleen, adipose tissue and eye, as well as the brain [30]. The MC4 receptor has also been found in some peripheral tissues in zebrafish [11]. The head kidney includes the inter-renal tissue, the piscean homologue to the adrenal gland. In mammals, it is the adrenal gland which is the predominant site for the expression of the MC2 receptor, which mediates the effects of ACTH on steroidoneogenesis. It is therefore possible that the expression of the MC4 receptor is reminiscent of a wider role of this receptor during early vertebrate evolution, and it is possible that the MC4 receptor participated in mediating the effect of ACTH on inter-renal tissues. This notion is also strengthened considering the relatively high affinity of the OmyMC4 receptor for ACTH. If this is true, it is possible that the MC4 receptor has subsequently developed into a more specific CNS receptor due to higher demand or requirement for the central regulation of body mass in the lineage leading to mammals.

In summary, we have shown that the rainbow trout has both MC4 and MC5 receptors. We have performed comprehensive characterization of their primary and 3D structures, pharmacology and tissue distribution. Interestingly, the rainbow trout receptors show several features that indicate that they may have shared functional roles during early vertebrate evolution. The receptor clones will facilitate functional characterization of the MC receptors in rainbow trout and our understanding of the roles of the genes involved in the complex MC system. The pharmacological characterization is important for further studies of the central regulation of food intake in rainbow trout. Moreover, the study provides important information in how MC receptors may have gained and lost their functions during the evolution of vertebrates.

We thank Christina Bergqvist for assistance with isolation of RNA and preparation of cDNA, and Dr Pierre Rescan (INRA, Rennes, France) for generously providing rainbow trout Lambda genomic library. J. K. was supported by the Wenner-Gren foundation and the European Union Marie Curie Fellowship programme. The studies were supported by the Swedish Research Council (VR, medicine), Swedish Research Council for Environment, Agricultural Sciences and Spatial Planning (FORMAS), the Swedish Society for Medical Research (SSMF), Svenska Läkaresällskapet, Åke Wikberg Foundation, The Novo Nordisk Foundation, Magnus Bergwall Foundation and Melacure Therapeutics AB, Uppsala, Sweden. T. H. was supported by the Federation of European Biochemical Societies (FEBS).

REFERENCES

1 Carroll, R. L. (1988) Vertebrate Paleontology and Evolution. WH Freeman and Co., New York
2 Nelson, J. C. (1994) Fishes of the World, 3rd edn, Wiley, New York
3 Thorgaard, G. H., Bailey, G. S., Williams, D., Buhler, D. R., Kaattari, S. L., Ristow, S. S., Hansen, J. D., Winton, J. R., Bartholomew, J. L., Nagler, J. J. et al. (2002) Status and opportunities for genomics research with rainbow trout. Comp. Biochem. Physiol. B. Biochem. Mol. Biol. **133**, 609–646
4 Schiöth, H. B. (2001) The physiological role of melanocortin receptors. Vitam. Horm. **63**, 195–232
5 Fredriksson, R., Lagerström, M. C., Lundin, L. G. and Schiöth, H. B. (2003) The G-protein-coupled receptors in the human genome form five main families: phylogenetic analysis, paralogon groups, and fingerprints. Mol. Pharmacol. **63**, 1256–1272
6 Chhajlani, V. (1996) Distribution of cDNA for melanocortin receptor subtypes in human tissues. Biochem. Mol. Biol. Int. **38**, 73–80
7 Chen, W., Kelly, M. A., Opitz-Araya, X., Thomas, R. E., Low, M. J. and Cone, R. D. (1997) Exocrine gland dysfunction in MC5-R-deficient mice: evidence for coordinated regulation of exocrine gland function by melanocortin peptides. Cell **91**, 789–798
8 Huszar, D., Lynch, C. A., Fairchild-Huntress, V., Dunmore, J. H., Fang, Q., Berkemeier, L. R., Gu, W., Kesterson, R. A., Boston, B. A., Cone, R. D. et al. (1997) Targeted disruption of the melanocortin-4 receptor results in obesity in mice. Cell **88**, 131–141
9 Fan, W., Boston, B. A., Kesterson, R. A., Hruby, V. J. and Cone, R. D. (1997) Role of melanocortinergic neurons in feeding and the agouti obesity syndrome. Nature (London) **385**, 165–168
10 Kask, A., Mutulis, F., Muceniece, R., Pahkla, R., Mutule, I., Wikberg, J. E., Rago, L. and Schiöth, H. B. (1998) Discovery of a novel superpotent and selective melanocortin-4 receptor antagonist (HS024): evaluation *in vitro* and *in vivo*. Endocrinology **139**, 5006–5014
11 Ringholm, A., Fredriksson, R., Poliakova, N., Yan, Y. L., Postlethwait, J. H., Larhammar, D. and Schiöth, H. B. (2002) One melanocortin 4 and two melanocortin 5 receptors from zebrafish show remarkable conservation in structure and pharmacology. J. Neurochem. **82**, 6–18
12 Klovins, J., Haitina, T., Fridmanis, D., Kilianova, Z., Kapa, I., Fredriksson. R., Gallo-Payet, N. and Schiöth, H. B. (2004) The melanocortin system in *Fugu*: determination of POMC/AGRP/MCR gene repertoire and synteny, as well as pharmacology and anatomical distribution of the MCRs. Mol. Biol. Evol. **21**, 563–579
13 Ringholm, A., Klovins, J., Fredriksson, R., Poliakova, N., Larson, E. T., Kukkonen, J. P., Larhammar, D. and Schiöth, H. B. (2003) Presence of melanocortin (MC4) receptor in spiny dogfish suggests an ancient vertebrate origin of central melanocortin system. Eur. J. Biochem. **270**, 213–221
14 Cerda-Reverter, J. M., Ringholm, A., Schiöth, H. B. and Peter, R. E. (2003) Molecular cloning, pharmacological characterization, and brain mapping of the melanocortin 4 receptor in the goldfish: involvement in the control of food intake. Endocrinology **144**, 2336–2349
15 Lagerström, M. C., Klovins, J., Fredriksson, R., Fridmanis, D., Haitina, T., Ling, M. K., Berglund, M. M. and Schiöth, H. B. (2003) High affinity agonistic metal ion binding sites within the melanocortin 4 receptor illustrate conformational change of transmembrane region 3. J. Biol. Chem. **278**, 51521–51526
16 Holst, B., Elling, C. E. and Schwartz, T. W. (2002) Metal ion-mediated agonism and agonist enhancement in melanocortin MC1 and MC4 receptors. J. Biol. Chem. **277**, 47662–47670
17 Larson, E. T., Fredriksson, R., Johansson, S. R. and Larhammar, D. (2003) Cloning, pharmacology, and distribution of the neuropeptide Y-receptor Yb in rainbow trout. Peptides **24**, 385–395
18 Thompson, J. D., Higgins, D. G. and Gibson, T. J. (1994) CLUSTAL W: improving the sensitivity of progressive multiple sequence alignment through sequence weighting, position-specific gap penalties and weight matrix choice. Nucleic Acids Res. **22**, 4673–4680
19 Reference deleted
20 Reference deleted
21 Palczewski, K., Kumasaka, T., Hori, T., Behnke, C. A., Motoshima, H., Fox, B. A., Le Trong, I., Teller, D. C., Okada, T., Stenkamp, R. E. et al. (2000) Crystal structure of rhodopsin: a G protein-coupled receptor. Science **289**, 739–745
22 Wold, S., Esbensen, K. and Geladi, P. (1987) Principal component analysis. Chemom. Intell. Lab. Syst. **2**, 37–52
23 Marklund, U., Bystrom, M., Gedda, K., Larefalk, A., Juneblad, K., Nystrom, S. and Ekstrand, A. J. (2002) Intron-mediated expression of the human neuropeptide Y Y1 receptor. Mol. Cell Endocrinol. **188**, 85–89

24 Schiöth, H. B., Muceniece, R. and Wikberg, J. E. (1996) Characterisation of the melanocortin 4 receptor by radioligand binding. Pharmacol. Toxicol. **79**, 161–165
25 Robinson-Rechavi, M., Marchand, O., Escriva, H., Bardet, P. L., Zelus, D., Hughes, S. and Laudet, V. (2001) Euteleost fish genomes are characterized by expansion of gene families. Genome Res. **11**, 781–788
26 Taylor, J. S., Van de Peer, Y., Braasch, I. and Meyer, A. (2001) Comparative genomics provides evidence for an ancient genome duplication event in fish. Philos. Trans. R. Soc. London Ser. B. **356**, 1661–1679
27 Huang, E. P. (1997) Metal ions and synaptic transmission: think zinc. Proc. Natl. Acad. Sci. U.S.A. **94**, 13386–13387
28 Assaf, S. Y. and Chung, S. H. (1984) Release of endogenous Zn^{2+} from brain tissue during activity. Nature (London) **308**, 734–736
29 Perez-Castejon, C., Vera-Gil, A., Barral, M. J., Perez-Castejon, M. J. and Lahoz, M. (1994) Zinc in hypothalamus and hypophysis of the rat. Histol. Histopathol. **9**, 259–262
30 Takeuchi, S. and Takahashi, S. (1998) Melanocortin receptor genes in the chicken – tissue distributions. Gen. Comp. Endocrinol. **112**, 220–231
31 Schiöth, H. B., Bouifrouri, A. A., Rudzish, R., Muceniece, R., Watanobe, H., Wikberg, J. E. and Larhammar, D. (2002) Pharmacological comparison of rat and human melanocortin 3 and 4 receptors *in vitro*. Regul. Pept. **106**, 7–12
32 Schiöth, H. B., Muceniece, R., Mutulis, F., Prusis, P., Lindeberg, G., Sharma, S. D., Hruby, V. J. and Wikberg, J. E. (1997) Selectivity of cyclic [D-Nal^{7}] and [D-Phe^{7}] substituted MSH analogues for the melanocortin receptor subtypes. Peptides **18**, 1009–1013
33 Schiöth, H. B., Muceniece, R., Wikberg, J. E. and Chhajlani, V. (1995) Characterisation of melanocortin receptor subtypes by radioligand binding analysis. Eur. J. Pharmacol. **288**, 311–317
34 Schiöth, H. B., Muceniece, R., Larsson, M. and Wikberg, J. E. (1997) The melanocortin 1, 3, 4 or 5 receptors do not have a binding epitope for ACTH beyond the sequence of α-MSH. J. Endocrinol. **155**, 73–78

Received 15 December 2003/9 February 2004; accepted 13 February 2004
Published as BJ Immediate Publication 13 February 2004, DOI 10.1042/BJ20031934